Influence of AlGaN n-type doping and AlN thickness on the two-dimensional electron gas density (n_s) and resistance (R_$2DEG$)

Clémentine Piotrowicz, Blend Mohamad, Nathalie Malbert, Marie-Anne Jaud, William Vandendaele, Matthew Charles, Romain Gwoziecki

Influence of AlGaN n-type doping and AlN thickness on the two-dimensional electron gas density (n_s) and resistance (R_{2DEG})

C. Piotrowicz*+, B. Mohamad*, N. Malbert+, M.-A. Jaud*, W. Vandendaele*, M. Charles*, R. Gwoziecki*

*CEA, LETI, MINATEC Campus, F-38054 Grenoble and Univ. Grenoble Alpes, F-38000 Grenoble, France
+University of Bordeaux, IMS Laboratory, CNRS UMR 5218, F-33400 Talence, France;
clementine.piotrowicz@cea.fr

Abstract

In this paper, electrical characterizations by $C(V_G)$ and $I_D(V_G)$ and comparison with 1D Schrödinger-Poisson simulations are carried out to investigate the effects of AlN layer thickness and n-type AlGaN barrier doping on the two-dimensional electron gas resistance (R_{2DEG}). Specifically, these impacts are related to either the electron sheet density (n_s) effects or the mobility (μ) effects. In this study, we show that varying the AlN thickness from 0.7nm (n_s=7.8cm^{-2}) to 1.5nm (n_s=9.0 cm^{-2}) leads to a linear increase of n_s. However, simultaneous degradation of the transport properties due to intensifying roughness mechanism at high n_s tend to limit the improvement of the device properties. Furthermore, we show that the heavily doped AlGaN barrier slightly increases n_s and drops the 2DEG mobility to ~1770 cm^2.V^{-1}.s^{-1} leading to a degraded 2DEG resistance. However, the overall resistance is improved (R=323Ω/□) compared to the undoped case (R=380Ω/□) due to the simultaneous contribution of two conducting channels at V_G=0V. To go further, the polarization charges at the AlGaN/AlN and AlN/GaN interfaces are computed in the 1D Schrödinger-Poisson simulations to account for the presence of the AlN layer. A reduced polarization for very thin AlN layers is considered to account for the experimental results. A very simple empirical model is proposed that predicts the enhancement of polarization charges (σ) as a function of AlN thickness.

Keywords: AlGaN/AlN/GaN heterostructure; 2DEG; AlN spacer; n-doped AlGaN; Schrödinger-Poisson simulations; Measurements.

1. Introduction

GaN High Electron Mobility Transistors (HEMTs) have attracted a lot of interest to improve the energy conversion system. The need to perform at a fast switching rate and high power density has pushed the research into ultra-wide bandgap materials such as GaN materials [1]. Indeed, III-N materials offer interesting properties due to their special würtzite crystal and polarization properties. The growth of AlGaN/GaN heterostructures leads to a high two-dimensional electron gas density (2DEG) to compensate for these interfaces polarization charges induced by the abrupt difference in polarization between GaN and AlGaN. This 2DEG and the high mobility properties of the III-V materials make them excellent candidates for power conversion applications. The efficiency of these conversion systems is related to the on-state resistance (R_{ON}) and consequently to the improvement of the 2DEG resistance. Firstly, the effect of the aluminum molar concentration in the $Al_xGa_{1-x}N$ barrier has been investigated and has shown that n_s enhancement is driven by Al-rich alloy concentration. This

has been directly correlated to the increase of the interfaces polarization charges with Al molar concentration[2]. AlGaN thickness optimization has also been investigated and it has been reported that its thickness increases n_s thanks to the different coupling capacitance effect.

In the interests of continuous improvement, a very thin AlN spacer has been added at the AlGaN/GaN heterojunction interface, with the aim of limiting the penetration of wave functions into the AlGaN barrier and thus improving the 2DEG mobility. However, experimental studies do not show an enhancement of n_s with 1nm AlN layer thickness compared to the conventional AlGaN/GaN heterojunction despite simulation studies report a large increase [3][4]. In this work, we will carry out a qualitative and quantitative comparison between measurements and simulations of the AlN thicknesses (0.7nm, 1.1nm and 1.5nm) impact on 2DEG n_s and mobility.

Another key parameter is the n-type doping of the AlGaN barrier. Indeed, at the beginning, it was believed that the high level of donors could enrich the 2DEG channel and consequently increase it leading to a lower R_{2DEG}. Contrary, in the very last state of the art studies, it is reported that the polarization mechanism prevails over the doping electrostatic effect [2] and therefore it has no effect on the n_s [3]. Moreover, it has been shown that AlGaN doping leads to mobility degradation due to impurity scattering in the AlGaN/GaN heterojunction. Here, we study the doping effect taking account of the thin AlN layer present at the heterojunction.

In this work, we will therefore attempt to give a comprehensive analysis of the AlN layer thickness and the effect of n-type AlGaN doping by comparing $C(V_G)$ and $I_D(V_G)$ measurements of normally on devices. These measurements will be compared to theoretical simulations of the capacitance. For the simulations, the 1D Schrodinger-Poisson equation the effective mass approximation (EMA) formalism for the Γ valley is considered.

2. Device structure and technology

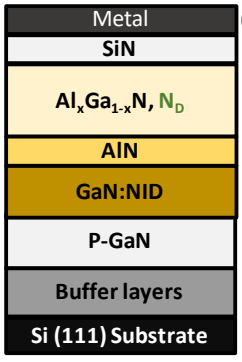

(b)

	t_{AlN} (nm)	N_D (cm^{-3})
A	0.7	NID
B	1.1	NID
C	1.5	NID
D	0.7	$1x10^{19}$

Figure 1 : (a) Cross-section of the studied structure. (b) Summary table of epitaxial variations.

The studied test structures are normally on devices, which means a two-dimensional electron gas (2DEG) is naturally present without external applied voltage. Indeed, this 2DEG onset occurs at the heterojunction AlGaN/AlN/GaN at V_G=0V. The overall stack structure is very complex to optimize due to the high quality GaN growth demand on a silicon substrate. The buffer layers consist of a few transition layers, which are used to reduce the lattice mismatch between Si and GaN, which is in the order of 17% [5], followed by a carbon-doped layer to decrease vertical leakage [6]. A p-GaN layer is then grown to ensure electrically neutral boundary conditions for our simulations and screen the substrate effect variability. 100nm of high-quality GaN NID (not intentionally doped) is grown on the top of the pGaN layer. The addition of a thin AlN layer at the interface of the well-known AlGaN/GaN heterojunction aims to increase the AlN/GaN band offset and the

device performance, as we will discuss in the following. $Al_xGa_{1-x}N$ epitaxy with about 23% aluminum molar concentration is then grown on the final heterojunction. On top, a SiN passivation layer, deposited by LPCVD, improves the device properties as reported in many studies [7] [8] [9]. In this paper, four epitaxial variations, shown in the table (Figure 1(b)), are investigated. Firstly, the impact of the AlN layer, varying from 0.7 to 1.5nm, is studied. Three samples are considered: 0.7nm (sample A), 1.1nm (sample B), and 1.5nm (sample C). In addition, the effect of an n-type AlGaN doped barrier for an AlN thickness of 0.7nm is also considered (sample D) in this study.

3. Polarization induced sheet charge density

These devices are based on III-N family materials which are well known for their strong spontaneous and piezoelectric polarization properties [10] [11]. Spontaneous polarization is naturally present in GaN, AlN, and AlGaN alloy material, and arises from the variation of the cation-anion bond length along the c-axis from the ideal structure. The internal cell parameter (u) is about 0.375 for the ideal würtzite structure. Due to this deviation from ideality in III-N materials, the u parameter is found, according to the work of Ambacher [12], to be 0.377 and 0.382 for the GaN and AlN respectively. This explains the higher spontaneous polarization of AlN (P_{sp}^{AlN}= -0.09 $C.m^{-2}$ and P_{sp}^{GaN}=-0.034 $C.m^{-2}$) compared to GaN. The piezoelectric polarization account for the deformation of the upper strained layer.

In Ambacher's work [1], spontaneous and piezoelectric polarization in AlGaN/GaN heterostructrures was investigated and the polarization charges were modeled. Here in this study, we extrapolate this theory to the AlGaN/AlN/GaN heterostructure, which includes the presence of the AlN layer. A schematic of this heterostructure with the polarization contributions of each layer is illustrated in Figure 2 for the Ga-polarity condition.

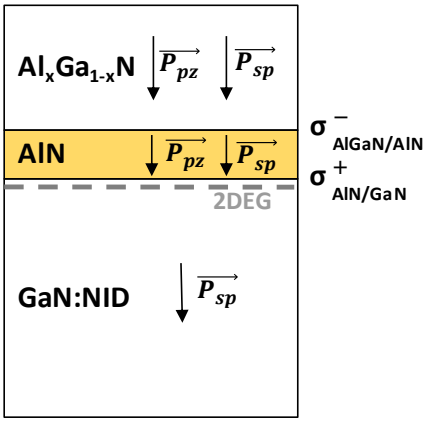

Figure 2 : Schematic of the spontaneous (P_{sp}) and piezoelectric (P_{pz}) polarizations inside the AlGaN/AlN/GaN heterostructure

The GaN material is assumed to be completely relaxed, so that no piezoelectric polarization occurs. Furthermore, the piezoelectric polarization of the AlGaN layer is calculated by assuming that the AlN thin layer ($t_{AlN} \in [0.7\ nm, 1.5\ nm]$) is fully constrained by the GaN layer as described by equation (1)

$$P_{pz}^{AlGaN}(x) = 2.d_{31}(x).\frac{a_{GaN}-a_{AlGaN}(x)}{a_{AlGaN}(x)}.\left(c_{11}(x)+c_{12}(x).\frac{c_{13}(x)^2}{c_{13}(x)}\right) \quad (1)$$

The rigidities and piezoelectric coefficients respectively d_{ij} and c_{ij} are calculated as a function of the molar concentration of aluminum content (x) using the Vegard's law as:

$$d_{ij}(x) = x.d_{ij}(AlN) + (1-x).d_{ij}(GaN) \quad (2)$$

$$c_{ij}(x) = x.c_{ij}(AlN) + (1-x).c_{ij}(GaN) \quad (3)$$

The spontaneous polarization in the $Al_xGa_{1-x}N$ as a function of x is calculated according to equation (4) where b is the bowing parameter taking equal to -0.021C.m^{-2}.

$$P_{sp}^{AlGaN}(x) = x.P_{sp}^{AlN} + (1-x).P_{sp}^{GaN} - b.x(1-x) \quad (4)$$

This leads to the definitions of dual polarization charges $\sigma_{AlN/GaN}$ and the $\sigma_{AlGaN/AlN}$ resulting from the polarization difference between the two materials at the interface; see equations (5) and (6) which are respectively positive and negative.

$$\sigma_{AlN/GaN} = \frac{1}{q}.\left\{P_{sp}^{GaN} - \left(P_{sp}^{AlN} + P_{pz}^{AlN}\right)\right\} \quad (5)$$

$$\sigma_{AlGaN/AlN} = \frac{1}{q}.\left\{\left(P_{sp}^{AlN} + P_{pz}^{AlN}\right) - \left(P_{sp}^{AlGaN} + P_{pz}^{AlGaN}\right)\right\} \quad (6)$$

The two-dimensional electron gas will form in the GaN layer at the AlN/GaN heterojunction to compensate the $\sigma_{AlN/GaN}$ charge which will be investigated in the remainder of this paper, The charge at the top between the AlGaN/SiN interface will be considered compensated [13].

4. Experimental Results

Figure 3, reports the current-voltage $I_D(V_G)$ and capacitance-voltage $C(V_G)$ characteristics for all the splits A, B, C and D.

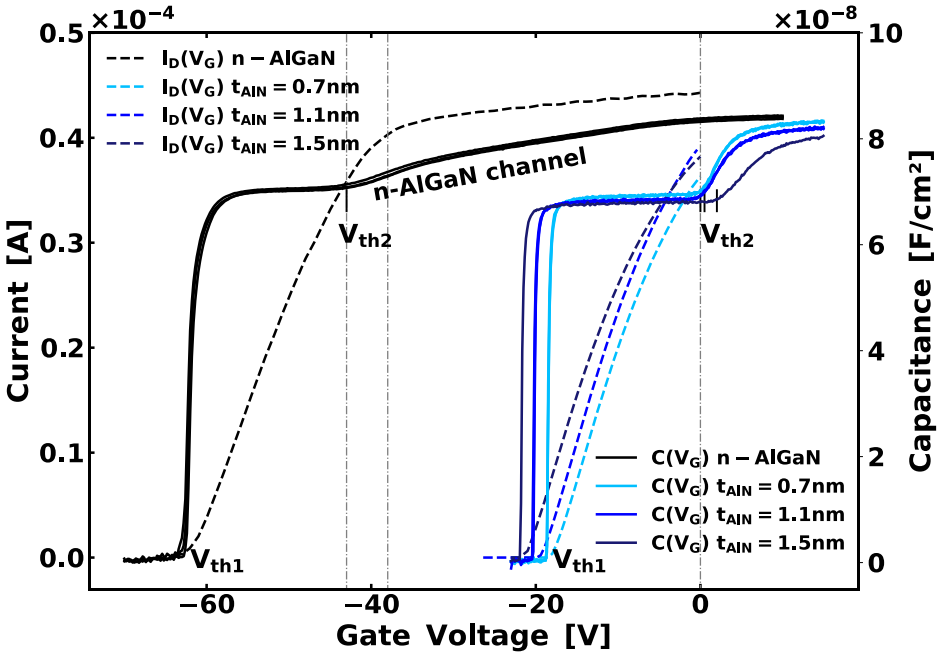

Figure 3: $I_D(V_G)$ and $C(V_G)$ measurements at 1kHz respectively on B1500 device analyzer and HP4284 LCR meter.

In the following, the first threshold voltage (V_{th1}) refers to the gate voltage condition for which the formation of 2DEG channel occurs in the GaN layer. The second threshold voltage (V_{th2}) refers to the second inversion channel formation occurring instead in the AlGaN layer. As reported in figure 3, $C(V_G)$ and $I_D(V_G)$ curves show that a V_{th1} shift toward negatives values is observed by increasing the AlN thickness layer, while for V_{th2} an opposite shift, towards positives values, is observed. Furthermore, when comparing sample A and D with the same AlN thickness but with n-type AlGaN doping for sample D, an important electrostatic shift toward large negative values is observed for both $C(V_G)$ and $I_D(V_G)$ curves. For what concerns specifically the $I_D(V_G)$ characteristics, by comparing the samples A, B and C at V_G=0V, the current does not increase by increasing t_{AlN} thickness with a clear dependency. Indeed, for value of 1.5 nm, a degradation of the current is observed. For sample D, the doped AlGaN layer leads to higher current level compared to the undoped cases (A, B and C). Concerning the $C(V_G)$ curves, similar maximum capacitances values are reported.

All the electrical parameters of AlGaN/AlN/GaN heterostructure such as n_s, R_{2DEG} and µ will be extracted at V_G=0V to characterize the 2DEG channel under normal conduction conditions of the MOS-HEMTs devices. The n_S is extracted from the $C(V_G)$ curves according to equation (7). The R_{2DEG} is calculated with equation (8) from the $I_D(V_G)$. Finally, the mobility is deduced using equation (9). For samples A, B and C, extractions at V_G=0V refer directly to 2DEG parameters while for the sample D, extractions at 0V refer to the contributions of both electron channels (GaN and AlGaN). The extraction results are reported in Figure 4(b). For sample D in figure 4(b), R_{2DEG}, n_s and µ are extracted at V_{th2} before the formation of the n-type AlGaN channel.

$$n_S\,(2DEG) = \frac{1}{q}\int_{V_{th1}}^{V} C.dV\Big|_{V=\begin{cases} 0\ if\ V_{th2}\geq 0V \\ V_{th2}\ if\ V_{th2}\ll 0V \end{cases}} \quad (7)$$

$$R_{2DEG,tot} = \frac{\pi}{ln(2)}.\frac{\Delta V}{I} \quad (8)$$

$$\mu_{S,tot} = \frac{1}{q.R_{2DEG,tot}.n_{S,tot}} \quad (9)$$

$$R_{AlGaN} = \frac{R_{tot}.R_{2DEG}}{R_{2DEG} - R_{tot}} \quad (10)$$

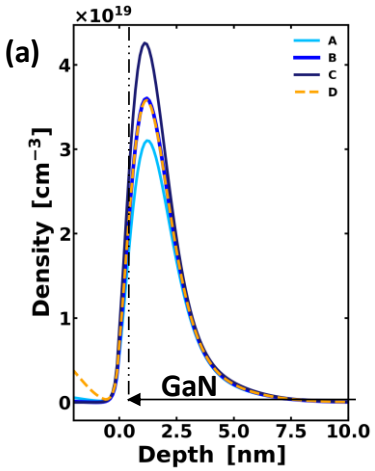

	n_S (cm^{-2})	R_{2DEG} (Ω/□)	μ_s ($cm^2.V^{-1}.s^{-1}$)
A	$7.8x10^{12}$	380	2103
B	$8.5x10^{12}$	344	2140
C	$9.0x10^{12}$	351	1981
D	$7.8x10^{12}$	452	1770

(b)

D	n_S (cm^{-2})	R (Ω/□)	μ ($cm^2.V^{-1}.s^{-1}$)
AlGaN channel	$2.1x10^{13}$	1457	202
2DEG	$8.5x10^{12}$	415	1770
Total	$2.9x10^{13}$	323	665

(c)

Figure 4: (a) Simulated 2DEG electron density profile for four samples at 15V gate voltage. (b) Extracted 2DEG parameters R_{2DEG}, n_s and μ_s at V_G=0V for samples A, B, C and at V_{th2} for sample D, (c) Detailed AlGaN and 2DEG channel parameters for sample D.

The n_s is find to increase linearly with the AlN thickness leading to a minimum resistance value at 1.1nm. Indeed, the degradation of the mobility at 1.5nm limits the further improvement on the resistance. In addition, for sample D, the n_s(2DEG) at V_{th2} is found to be similar to sample A, which differ only by the AlGaN doped barrier. In figure 4(a), we report also the simulated 2DEG density as a function of the depth across the heterojunction. These results confirm the increase of n_s with the AlN thickness but it also show that n_s increases for sample D compared to sample A. The slight variation of the 2DEG value obtained by simulation compared to the experimental extraction is explained by the simultaneous variations of both channels after the V_{th2} value, which was not taken into account during the experimental extraction.

In figure 4(c), new n_s(2DEG) is extracted taking into account of the second electron channel density for $V_G > V_{th2}$. The new R_{2DEG} value is lower than the one extracted at V_{th2} due to the increase of the 2DEG density. The total resistance decreases to 323 Ω /□ due to the high level of donors in the AlGaN. Finally, R_{AlGaN} is determined using equation (10).

5. Electron density and mobility

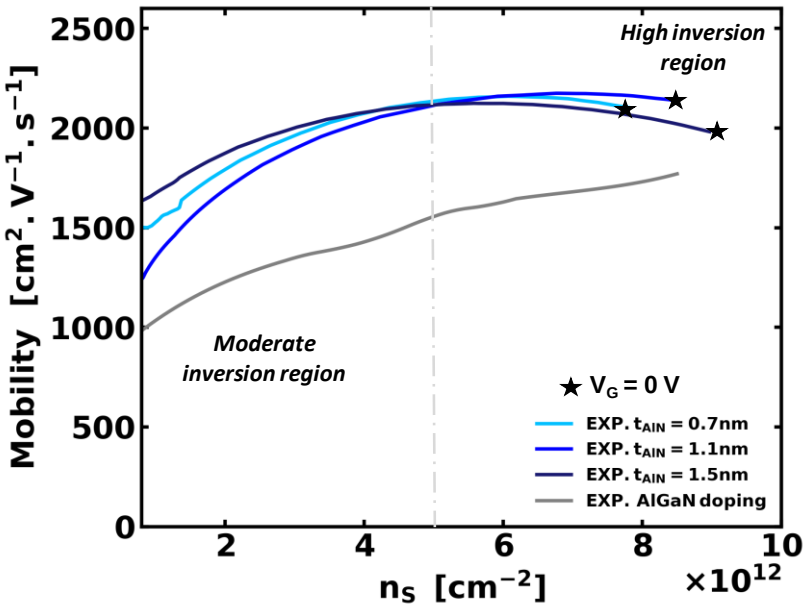

Figure 5: Extracted effective 2DEG mobility as a function of the electron density for sample A, B, C and D.

For a deep insight of n_s, μ and R correlations and their associate limiting mechanisms, figure 5 reports the experimental 2DEG mobility as a function of the electron density n_S. Two regimes are depicted, the moderate inversion ($n_S < 5x10^{12}cm^{-2}$) and the strong inversion ($n_S > 5x10^{12}cm^{-2}$). Concerning the AlN thickness impact at moderate inversion, no linear dependency with the mobility is observed. Indeed, at first, a degradation of the mobility is observed passing from 0.7 to 1.1nm thickness value but then an improvement of the mobility occurs at 1.5nm value. The opposite is observed at strong inversion, where the most deteriorated mobility is associated to the 1.5nm AlN thickness. By considering these mobility effects and their non-linearity with the AlN thickness, the minimum and optimal resistance value, at strong inversion, is found to be at 1.1nm, identified as the best trade-off between these mobility and n_s conditions.

In figure 6, we report the simulations results of the energy conduction bands and the 2DEG electron density as a function of the heterojunction depth for the four splits. The case of an AlGaN/GaN simple heterojunction has also been simulated and it confirms the benefit of the AlN spacer layer to eliminate the wavefunctions

penetration in the AlGaN. In other studies they also assume that the AlN spacer tend to reduce the effect of the AlGaN alloy scattering mechanism on the 2DEG responsible for mobility deterioration [14] [15]. I. P. Smorchkova's work confirms experimentally an increase in the 2DEG mobility by the addition of this thin 1nm AlN spacer at the interface of the AlGaN/GaN heterostructure. Another study also reported no increase in n_s [16]. In this article, the mobility degradation observed at thicker AlN (1.5nm) layer could be associated to enhanced roughness mechanism. Indeed, the degradation of the mobility occurs also through roughness even between binary compounds. This effect is even enhance with higher values of polarization charges that tends to push the 2DEG near the heterojunction as it is highlighted in figure 6 [17] [18]. Another assumption explaining the mobility degradation is enhanced scattering mechanism due to dislocations with larger AlN layer coming from the significant lattice mismatch between AlN and GaN has reported by X. Han *et al.* [19]

Concerning the n-type AlGaN-doping barrier as reported in Fig. 5, an overall degradation of the mobility is observed for moderate and strong inversion. This is due to coulomb scattering because of the high level of donor doping presence within 1 to 5 nm GaN channel. Exhaustive mobility calculations would provide enhance expertise on the quantitative effect of each mechanism on this mobility degradation.

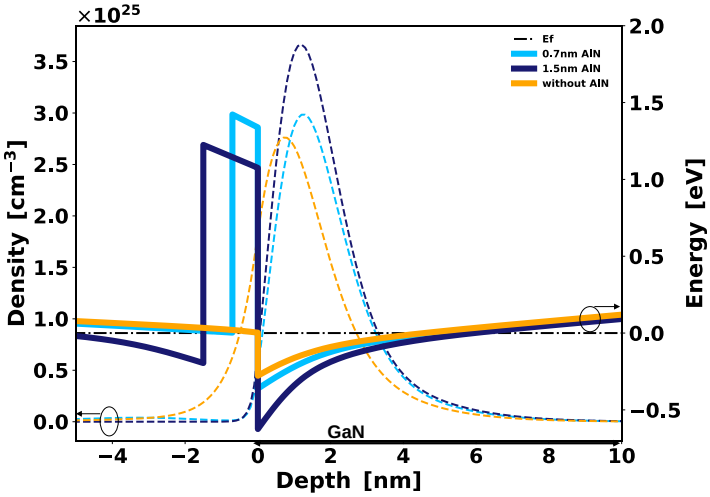

Figure 6: 1D Schrödinger-Poisson simulations of the 2DEG electron density and the energy conduction bands versus the depth. Two types of heterojunction are considered the AlGaN/GaN (in yellow) and the AlGaN/AlN/GaN with two AlN thickness (in blue).

6. 1D Schrödinger-Poisson simulations

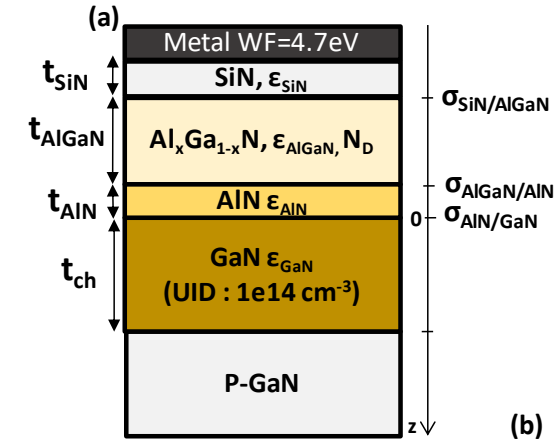

	Metal	SiN	AlGaN	AlN	GaN
WF(eV)	4.7	-	-	-	-
E_G (eV)	-	5.0	3.88	6.16	3.44
χ (eV)	-	1.9	3.22	1.80	3.50
ε_r	-	7.0	10.29	10.31	10.28

Figure 7: (a) Simulated structure, (b) Material parameters

The schematized structure in figure 7(a) is simulated by solving self-consistently the 1D Schrödinger-Poisson equations under the parabolic mass approximation for the Γ-valley. Wavefunction penetrations is also considered in the heterostructure. The material parameters are taken from reference [13], and recalled in figure 7(b). The thicknesses of AlGaN (t_{AlGaN}) and SiN (t_{SiN}) are extracted plotting Q_{inv}/C_{exp} as a function of Q_{inv} (Fig 8) [20] and then, from these extrapolated values, adjusted to fit the experimental capacitances (splits A, B, C and D).

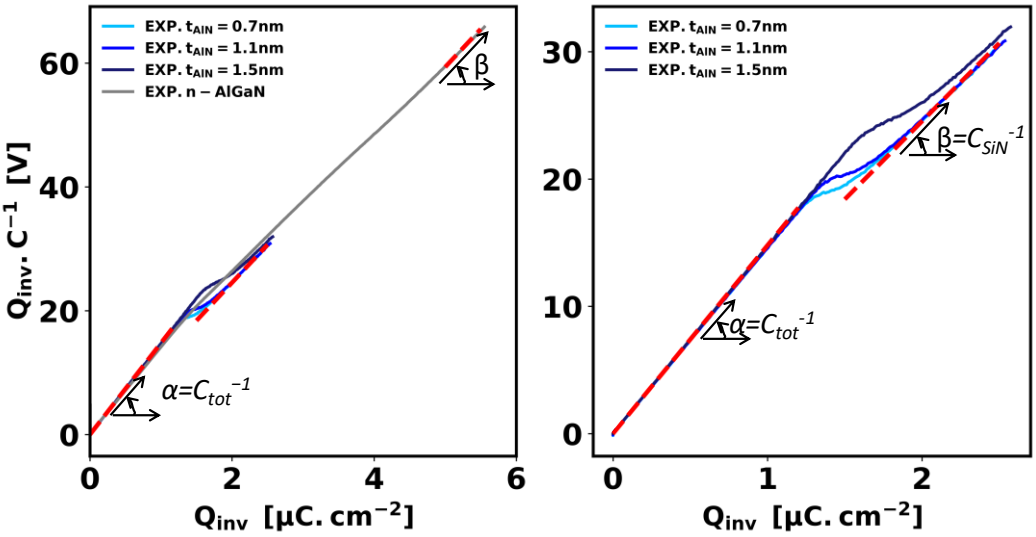

Figure 8: (a) Experimental $Q_{inv}.C^{-1}$ versus Q_{inv} method for the extraction of the AlGaN and SiN thicknesses

$$\beta = C_{SiN}^{-1} = \frac{\varepsilon_{SiN}}{t_{SiN}} \qquad (11)$$

$$\alpha = C_{tot}^{-1} = C_{AlGaN}^{-1} + C_{AlN}^{-1} + C_{SiN}^{-1} \qquad (12)$$

Moreover, the back-barrier condition in the p-GaN layer is determined experimentally according to the previous work [13]. Indeed, the electrostatic shift observed by varying t_{ch} on the C(V_G) curves, allows to extract the most appropriate value for the equivalent doping concentration.

Figure 9, shows the effect of the AlN thickness on the simulated C(V_G) by computing the charges $\sigma_{AlN/GaN}$ and $\sigma_{AlGaN/AlN}$ calculated using equations (5) and (6) which assume complete polarization. The experimental trend on V_{th1} and V_{th2} is reproduced, however the effect of the AlN layer is overestimated compared to the experimental C(V_G). Indeed, V_{th1} values are find too negative and V_{th2} values too positive compared to the experimental characteristics. In order, to reproduce the experimental behavior, $\sigma_{AlN/GaN}$ and $\sigma_{AlGaN/AlN}$ are adjusted to account for the experimental V_{th1} and V_{th2}.

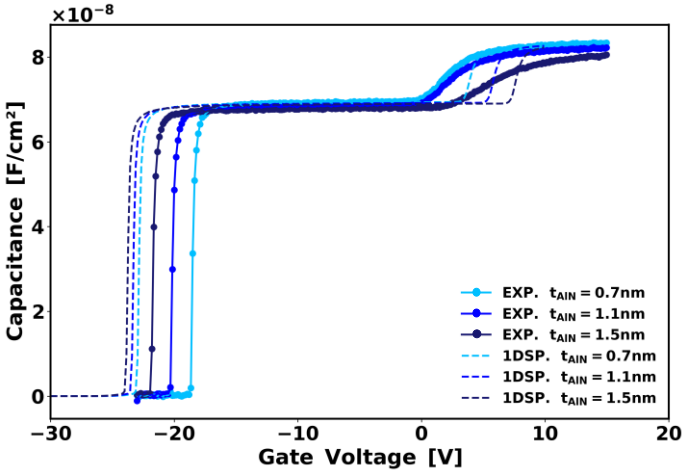

Figure 9: Effect of the AlN layer thickness on the C(V_G) simulations, considering the calculated charges from equations 5 and 6.

Figure 10(a) shows the simulations results compared to the experimental C(V_G) and figure 10(b) recalled the fitting charges for all samples. $\sigma_{AlN/GaN}$ and $\sigma_{AlGaN/AlN}$ values are found to be respectively reduced and increased as AlN thickness increases but also to be underrated compared to the value obtained using equations (5) and (6). In Figure 11, we report the associate electron densities as a function of thickness across the structure at different V_G conditions. They confirm the experimental effects observed on n_s. Indeed, as AlN thickness increases, the polarization charges are as well increased leading to an increased n_s and to a larger negative V_{th1} (sample A, B and C).

On the other hand, as reported in Fig 10(d), considering the doped AlGaN barrier with an AlN of 0.7nm, the electron channel in the AlGaN forms earlier at very large negative V_G conditions before 0V. This earlier formation is explained by the electrostatic effect induced by the high volume-doping concentration in the whole AlGaN layer. Moreover, for V_G values very close to V_{th2}, the formation of the AlGaN channel is associated by a further slight increase of the 2DEG as shown in figure 10(d). This is linked to the formation of the AlGaN channel at the AlGaN/AlN interface, therefore very close to the 2DEG channel. The progressive filling of the AlGaN layers by electrons for values higher than V_{th2} explains the experimental capacitance characteristic trend for the doped case (Sample D). Indeed, the progressive delocalization of the AlGaN electron channel barycenter

form the AlGaN/AlN to the SiN/AlGAN interface give meaning to a less abrupt capacitance characteristic compared to the undoped cases (A, B and C). More importantly, it is worth to mention that the same polarization charges found in case A have been considered for the doped AlGaN barrier to account for the V_{th1} and V_{th2} and to explain the experimental result.

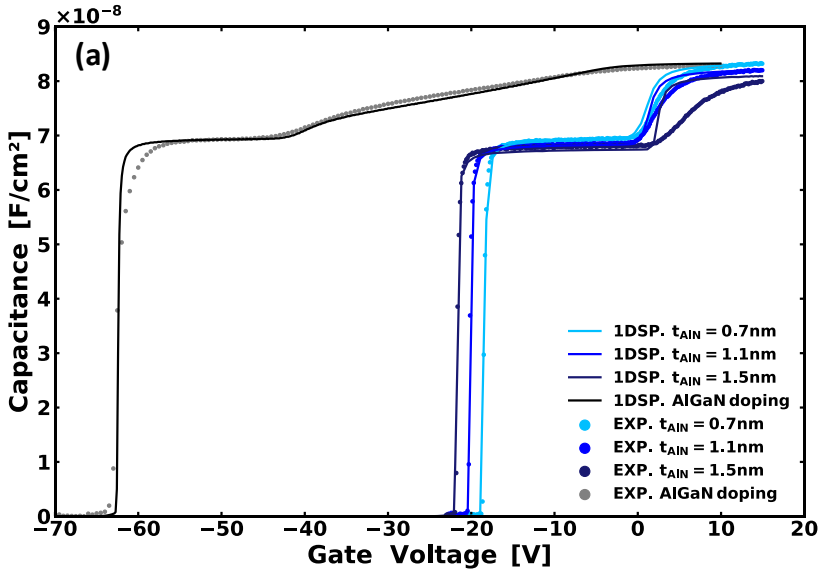

(b)	$\sigma_{AlGaN/AlN}$ (cm^{-2})	$\sigma_{AlN/GaN}$ (cm^{-2})
A	-6.00×10^{12}	1.57×10^{13}
B	-8.00×10^{12}	1.82×10^{13}
C	-1.42×10^{12}	2.5×10^{13}
D	-6.00×10^{12}	1.57×10^{13}

Figure 10: (a) $C(V_G)$ simulations (lines) and comparison with the experimental $C(V_G)$ (dots) for samples A, B, C and D; (b) Implemented interfaces charges to account for the experimental results in 1D Schrödinger-Poisson resolutions

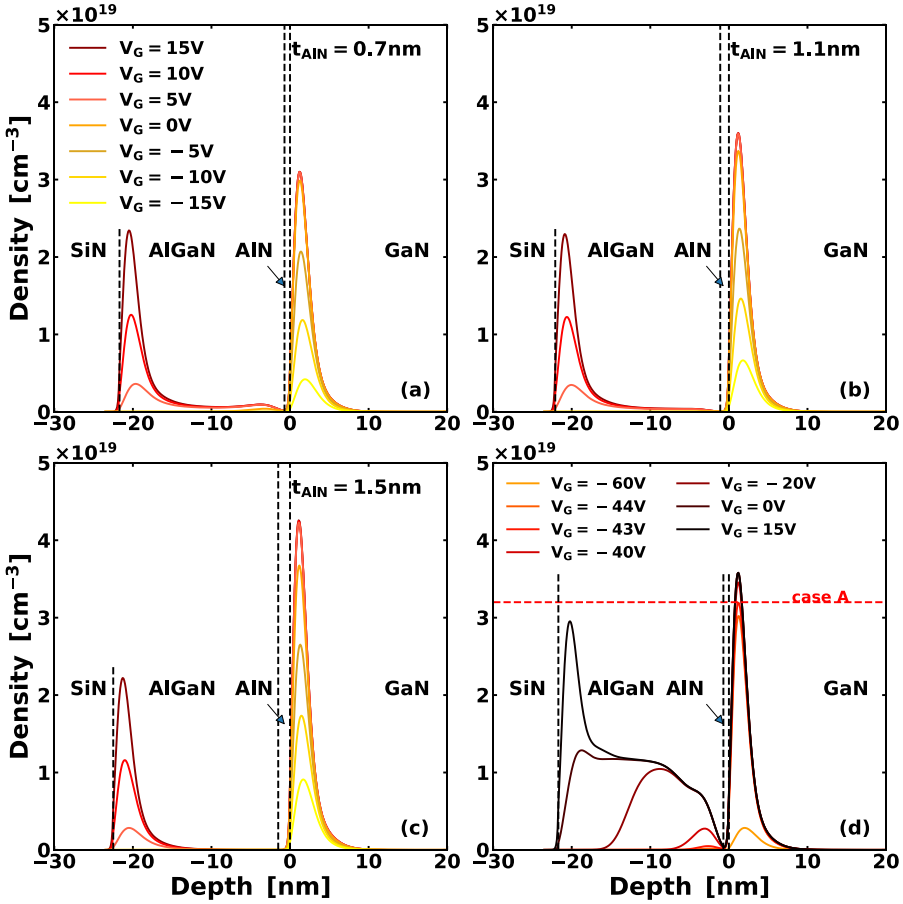

Figure 11: Electron density versus Depth at various V_G obtained from 1DSP simulations, (a) for t_{AlN}=0.7nm, (b) for t_{AlN}=1.1nm, (c) for t_{AlN}=1.5nm, (d) for the n-doped AlGaN, t_{AlN}=0.7nm.

As the polarization charges are found underrated with thinner AlN layers compared to Ambacher's model prediction, a model based on a reduced polarization is proposed. The parameter PR, being the reduced polarization factor, is implemented in the $\sigma_{AlN/GaN}$ and $\sigma_{AlGaN/AlN}$ equations, respectively (13) and (14). In figure 12, the theoretical polarization charges are plot as a function of PR (solid line for $\sigma_{AlN/GaN}$ and dashed line for $\sigma_{AlGaN/AlN}$). In addition, we report the experimental PR calculated for each polarization charge from figure 9(b) (symbols). The associate PR values for $\sigma_{AlN/GaN}$ and $\sigma_{AlGaN/AlN}$ are found to be similar, within 3% of variation, for each AlN thickness. Moreover, PR increases as AlN thickness increases. This trend includes also the sample D, with the AlGaN doped layer, where the same PR as for sample A is extracted. Figure 13 reports the PR as a function of the AlN thickness for all the samples. Two points are also reported: one from Berdalovik's work [21], which assumes 65% polarization for 3.5nm AlN to account its experimental results and the second from the Ambacher's work which consider a complete polarization for the polarization charges calculations at 30nm AlN thickness[2].

$$\sigma_{AlN/GaN} = \frac{1}{q}.\left\{P_{sp}^{GaN} - \left(P_{sp}^{AlN} + P_{pz}^{AlN}\right) \times PR\right\} \quad (13)$$

$$\sigma_{AlGaN/AlN} = \frac{1}{q}.\left\{\left(P_{sp}^{AlN} + P_{pz}^{AlN}\right) \times PR - \left(P_{sp}^{AlGaN} + P_{pz}^{AlGaN}\right)\right\} \quad (14)$$

$$PR = 1 - e^{\left(-0.117 \times t^2 + 4.164\right)} \quad (15)$$

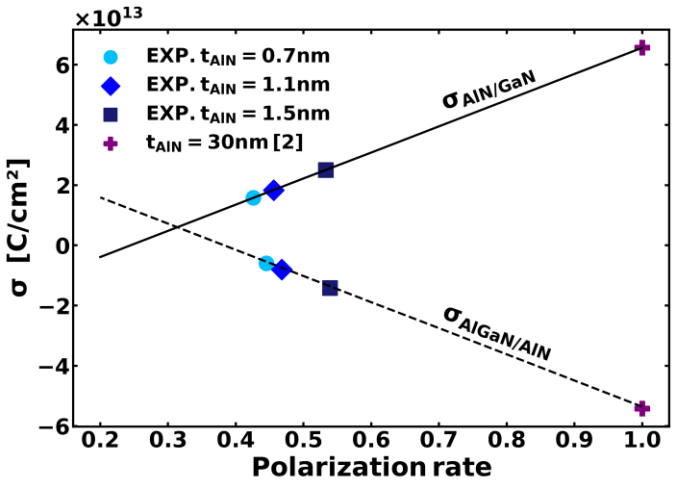

Figure 12: Lines: $\sigma_{AlGaN/AlN}$ and $\sigma_{AlN/GaN}$ vs PR (Eq.6-7). Dots: $\sigma_{AlGaN/AlN}$ and $\sigma_{AlN/GaN}$ extracted from measurements.

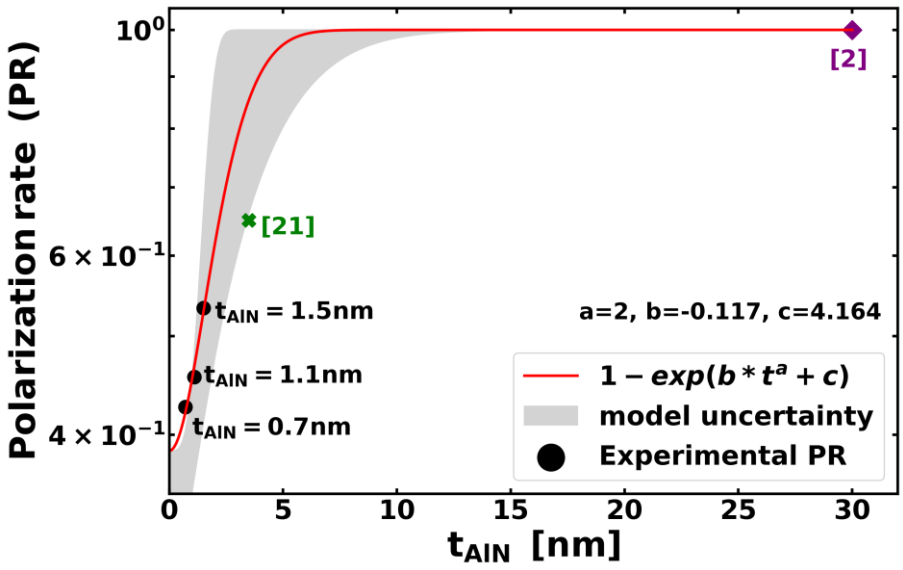

Figure 13: Empirical model predicting the evolution of the polarization rate in the AlN layer as a function of its thickness

An empirical model is proposed (15) to reproduce the experimental trend reported in Fig. 13, where a, b and c are respectively the fitting parameters. The observed reduction of the polarization as a function of the AlN thickness can be the cause of a compensation effect between $\sigma_{AlN/GaN}$ and $\sigma_{AlGaN/AlN}$. This assumption is valid

only for very thin thickness (≤0.7nm) to understand the trend on V_{th1}. Indeed, the variation of this $\sigma_{AlGaN/GaN}$ charge as affect only on V_{th1}, yet, the V_{th2} varie with the AlN thickness as we see in simulations and experimental measurements in figures 8 and 9(a). For consequences, the charge $\sigma_{AlGaN/AlN}$ is crucial to consider the AlN effect, and we are not allowed to neglected the AlN for larger thickness.

Another hypothesis is the quality of AlN, if the polarization seems reduced maybe the AlN layer is not pure AlN but some rich Al-layer. However, in B. Mazumder *et al.*, they demonstrated growth of pure Al for 2nm [22]. The charge might be compensated by some interface defects with the growth of an AlN layer with larger lattice mismatch than the AlGaN. This phenomenon was reported by X. Han *et al*, who explained the reduction in mobility within a larger AlN layer by the increase in interface dislocations induced by the increase in tensile strain[19]. The explanation is still misunderstood, but the model of reduced polarization seems to give nice approximations for model.

7. Conclusions

A comprehensive analysis of AlN thickness and n-type doping AlGaN layer on 2DEG resistance has been carried out by comparing $C(V_G)$ and $I_D(V_G)$ measurements with 1D Schrödinger-Poisson simulations. We have shown that the n-type AlGaN doping barely increase the 2DEG density and degrades the 2DEG mobility even with the presence of a thin AlN layer. However, the high level of doping leads to an overall resistance reduction due to the participation of two conductive channels (AlGaN, GaN). Concerning the effect of the AlN layer thickness, we have reported a linear increase of n_s with thicker AlN layer. This increase is justified by the enhancement of the interface polarization charges at both AlGaN/AlN and AlN/GaN interfaces. To take into account of this enhancement, we have assumed incomplete polarization for very thin AlN layer. The origin of this incomplete polarization is however still unknown. Additionally, the improvement of the 2DEG resistance is driven by n_s and μ enhancement. Thereby, by considering the mobility degradation mechanism appearing at 1.5nm AlN thickness, assumed linked to the interface roughness or scattering mechanism due to dislocations, we have found that AlN thickness at 1.1nm lead to the minimal R_{2DEG} resistance. Finally, a simple empirical model is proposed for device simulations taking into account of this thin AlN layer.

Acknowledgments

The authors would like to acknowledge the funding support from the PSPC French national program « G-Mobility ».

REFERENCES

[1] T. J. Flack, B. N. Pushpakaran, and S. B. Bayne, 'GaN Technology for Power Electronic Applications: A Review', *J. Electron. Mater.*, vol. 45, no. 6, pp. 2673–2682, Jun. 2016, doi: 10.1007/s11664-016-4435-3.

[2] O. Ambacher *et al.*, 'Two dimensional electron gases induced by spontaneous and piezoelectric polarization in undoped and doped AlGaN/GaN heterostructures', *J. Appl. Phys.*, vol. 87, pp. 334–344, 2000, doi: 10.1063/1.371866.

[3] F. Sonmez *et al.*, 'The effect of barrier layers on 2D electron effective mass in Al0.3Ga0.7N/AlN/GaN heterostructures', *J. Phys. Condens. Matter*, vol. 33, p. 255501, 2021, doi: 10.1088/1361-648x/abf8d2.

[4] N. M. Shrestha, Y. Li, and E. Y. Chang, 'Simulation study on electrical characteristic of AlGaN/GaN high electron mobility transistors with AlN spacer layer', *Jpn. J. Appl. Phys.*, vol. 53, no. 4 SPEC. ISSUE, 2014, doi: 10.7567/JJAP.53.04EF08.

[5] A. Krost and A. Dadgar, 'GaN-based optoelectronics on silicon substrates', pp. 77–84, May 2002.

[6] A. Fariza *et al.*, ‘Leakage currents and Fermi-level shifts in GaN layers upon iron and carbon-doping’, *J. Appl. Phys.*, vol. 122, no. 2, p. 025704, Jul. 2017, doi: 10.1063/1.4993180.
[7] A. Asgari and L. Faraone, ‘SiN passivation layer effects on un-gated two-dimensional electron gas density in AlGaN/AlN/GaN field-effect transistors’, *Appl. Phys. Lett.*, vol. 100, p. 122106, 2012, doi: 10.1063/1.3696641.
[8] M. Miczek, C. Mizue, T. Hashizume, and B. Adamowicz, ‘Effects of interface states and temperature on the C-V behavior of metal/insulator/AlGaN/GaN heterostructure capacitors’, *J. Appl. Phys.*, vol. 103, p. 104510, 2008, doi: 10.1063/1.2924334.
[9] A. Siddique, R. Ahmed, J. Anderson, M. Holtz, and E. L. Piner, ‘Improved Electrical Properties of AlGaN/GaN High-Electron-Mobility Transistors by In Situ Tailoring the SiNx Passivation Layer’, *ACS Appl. Mater. Interfaces*, vol. 13, pp. 18264–18273, 2021, doi: 10.1021/acsami.1c01241.
[10] F. Bernardini and V. Fiorentini, ‘Spontaneous versus Piezoelectric Polarization in III–V Nitrides: Conceptual Aspects and Practical Consequences’, *Phys. Status Solidi B*, vol. 216, no. 1, pp. 391–398, 1999, doi: 10.1002/(SICI)1521-3951(199911)216:1<391::AID-PSSB391>3.0.CO;2-K.
[11] F. Bernardini and V. Fiorentini, ‘Nonlinear macroscopic polarization in III-V nitride alloys’, *Phys. Rev. B*, vol. 64, no. 8, p. 085207, Aug. 2001, doi: 10.1103/PhysRevB.64.085207.
[12] O. Ambacher *et al.*, ‘Pyroelectric properties of Al(In)GaN/GaN hetero- and quantum well structures’, *J. Phys. Condens. Matter*, vol. 14, pp. 3399–3434, 2002, doi: 10.1088/0953-8984/14/13/302.
[13] B. Rrustemi *et al.*, ‘Investigation on interface charges in SiN/AlxGa1−xN/GaN heterostructures by analyzing the gate-to-channel capacitance and the drain current behaviors’, *J. Appl. Phys.*, vol. 130, no. 10, 2021, doi: 10.1063/5.0058019.
[14] G. Bastard, *Wave Mechanics Applied to Semiconductor Heterostructures*, Les Editions de Physique. Les Ulis, 1988.
[15] L. Hsu and W. Walukiewicz, ‘Effect of polarization fields on transport properties in AlGaN/GaN heterostructures’, *J. Appl. Phys.*, vol. 89, no. 3, p. 1783, 2001, doi: 10.1063/1.1339858.
[16] I. P. Smorchkova *et al.*, ‘AlN/GaN and (Al,Ga)N/AlN/GaN two-dimensional electron gas structures grown by plasma-assisted molecular-beam epitaxy’, *J. Appl. Phys.*, vol. 90, no. 10, pp. 5196–5201, Nov. 2001, doi: 10.1063/1.1412273.
[17] A. Gold, ‘Electronic transport properties of a two-dimensional electron gas in a silicon quantum-well structure at low temperature’, *Phys. Rev. B*, vol. 35, no. 2, pp. 723–733, Jan. 1987, doi: 10.1103/PhysRevB.35.723.
[18] D. Ferry, S. M. Goodnick, *Transport In Nanostructures*. CAMBRIDGE UNIVERSITY PRESS, 1997.
[19] X. Han *et al.*, ‘Scattering times in the two-dimensional electron gas of Al $_x$ Ga $_{1-x}$ N/AlN/GaN heterostructures’, *J. Phys. Appl. Phys.*, vol. 42, no. 4, p. 045112, Feb. 2009, doi: 10.1088/0022-3727/42/4/045112.
[20] I. Ben Akkez *et al.*, ‘New parameter extraction method based on split C-V for FDSOI MOSFETs’, in *2012 Proceedings of the European Solid-State Device Research Conference (ESSDERC)*, Sep. 2012, pp. 217–220. doi: 10.1109/ESSDERC.2012.6343372.
[21] I. Berdalovic, M. Poljak, and T. Suligoj, ‘A comprehensive model and numerical analysis of electron mobility in GaN-based high electron mobility transistors’, *J. Appl. Phys.*, vol. 129, no. 6, p. 064303, Feb. 2021, doi: 10.1063/5.0037228.
[22] B. Mazumder, M. H. Wong, C. A. Hurni, J. Y. Zhang, U. K. Mishra, and J. S. Speck, ‘Asymmetric interfacial abruptness in N-polar and Ga-polar GaN/AlN/GaN heterostructures’, *Appl. Phys. Lett.*, vol. 101, no. 9, p. 091601, Aug. 2012, doi: 10.1063/1.4748116.